

## Thermomechanical and Shape Memory Properties of SCF/SBS/LLDPE Composites\*

Yong-kun Wang<sup>a\*\*</sup>, Wen-chao Tian<sup>a</sup>, Guang-ming Zhu<sup>b</sup> and Jian-qiang Xie<sup>c</sup>

<sup>a</sup> Key Laboratory of Ministry of Education for Electronic Equipment Structure Design, Xidian University, Xi'an 710071, China

<sup>b</sup> Department of Applied Chemistry, Northwestern Polytechnical University, Xi'an 710129, China

<sup>c</sup> Department of Polymer materials and Engineering, College of Material Science and Engineering, North China University of Science and Technology, Tangshan 063009, China

**Abstract** A thermally triggered shape memory polymer composite was prepared by blending short carbon fiber (SCF) into a blend of poly(styrene-*b*-butadiene-*b*-styrene) triblock copolymer (SBS)/linear low density polyethylene (LLDPE) prior to curing. These composites have excellent processability compared with other thermosets. The dynamic mechanical analysis (DMA) and differential scanning calorimetry (DSC) were investigated to assess the thermomechanical properties of the SCF/SBS/LLDPE composite. Scanning electron microscope (SEM) imaging of the samples was performed to show the distribution of the SCF in the composite. The study specifically focused on the effect of SCF on the shape memory behavior of the SCF/SBS/LLDPE composite. The results indicated that the large amount of SCF significantly improved the mechanical property of the polymer composites while not damaging the shape memory performance. The SCF/SBS/LLDPE composites exhibited excellent shape memory behavior when the SCF content was less than 15.0 wt%. Moreover, the shape fixity ratio and shape recovery time of the SCF/SBS/LLDPE composites increased with the SCF content.

**Keywords:** Short carbon fiber; SCF/SBS/LLDPE composite; Mechanical properties; Shape memory behavior.

### INTRODUCTION

Shape memory polymers (SMPs) are stimuli-responsive materials that can “remember” their original shape upon exposure to external stimuli such as light, electric fields, magnetic fields, pH-values, or solvents<sup>[1–7]</sup>. SMPs have attracted great attention to scientists and engineers for this reason. These materials can be transformed and then “recovered” to their original shape above a certain transition temperature. Compared to shape memory metallic alloys and shape memory ceramics, SMPs possess the advantage of light weight, low cost, good processability, high shape recoverability and tunable shape memory transition temperature<sup>[8]</sup>. Therefore, they are ideal candidates for applications in different fields including, for instances, smart textiles and apparels, heat shrinkable packaging, intelligent biomedical materials, self-deployable structures in satellites and morphing wing structures<sup>[9–12]</sup>.

The SMP composites have received considerable attention over the last decade due to their scientific and technological barriers, such as lower mechanical strength and shape recovery stress, all these prevent their widespread applications and development. Thus, SMP composites have been developed. The SMP composites were usually prepared by using high modulus inorganic or organic fillers to reinforce pristine SMPs. However, it

\* This work was financially supported by the National Natural Science Foundation of China (No. 51403050) and Fundamental Research Funds for the Central Universities of China (Nos. JB150408 and XJS15021).

\*\* Corresponding author: Yong-kun Wang (王永坤), E-mail: ykwang@xidian.edu.cn

Received April 20, 2016; Revised May 12, 2016; Accepted May 19, 2016

doi: 10.1007/s10118-016-1838-9

has been observed that there is a trade-off between enhancement of modulus and reduction of shape memory. Generally, fillers exert negative impact on recoverable strain due to their size and substantially higher stiffness compared to the matrix polymer. Consequently, numerous efforts have been made to strike a balance between the recovery stress and recovery strain by use of fillers. Zhang *et al.*<sup>[13]</sup> filled shape memory polyurethane (SMPU) with microfiber. It was found that the microfiber SMPU film afforded much quicker and sharper shape recovery compared to the bulk SMPU. The quick shape recovery of the microfiber SMPU film was considered to be due to the high surface area of microfiber film that favorable for quicker heating/cooling of the sample and quicker diffusion of water. Lu *et al.*<sup>[14]</sup> investigated the shape memory behavior of carbon black and short carbon fibers reinforced styrene-based shape memory resin. Their results showed that the mechanical resistive loading and thermal conductivity of a composite (with hybrid filler content of 7.0 wt%) were improved by 160% and 200%, respectively, in comparison with those of pure bulk SMP. Lan *et al.*<sup>[15]</sup> studied the performance of carbon fiber fabric reinforced composite based on styrene-based SMP. It was found that the SMPC presented a higher storage modulus than the pure SMPs. The shape recovery ratio of the SMPC was above 90% at/above shape transition temperature, and the primary mechanism in the bending deformation of SMPC was believed to be the microbuckling.

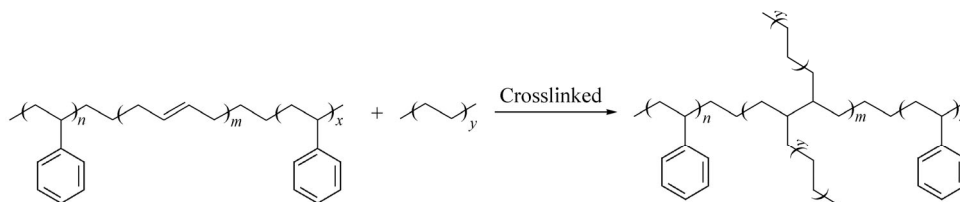
In this paper, cross-linked poly(styrene-*b*-butadiene-*b*-styrene) triblock copolymer (SBS)/linear low density polyethylene (LLDPE) is reinforced by short carbon fiber, and a new type of shape memory polymer composite is developed. The main objective is to systematically characterize the shape recovery properties of the SMPC, in order for the SMPC to meet the needs of the engineering application. Our focuses include the basic mechanical performances, shape recovery performances and microstructural deformation mechanisms.

## EXPERIMENTAL

### Materials and Preparation

SBS (PS/PB = 30/70,  $M_n = 1.05 \times 10^5$ ) was purchased from Balin Petroleum Chemical Corporation, Sinopec Group, China. LLDPE ( $M_n = 5 \times 10^4$ ) was produced by Tianjin Petro-Chemical Corp, China. SCF (Yancheng City Xiangsheng Carbon Fiber Technology Co. Ltd., approximately 30 mm in length and 7  $\mu\text{m}$  in diameter) was obtained by continuous cutting of carbon fiber. These materials were used as received.

SBS, LLDPE, SCF and dicumyl peroxide (DCP, 0.1 wt%) were blended in a Banbury mixer (PLE 651, Brabender, Germany) at 130 °C for 10 min (SBS/LLDPE = 70/30). The samples were then compressed into plates in a hot press at 160 °C with a pressure of 10 MPa. In the blends, the DCP was used to initiate the cross-linking between SBS and LLDPE to form an interpenetrating of hard and soft phase condensed state structure SMP material (Scheme 1). After the curing process, the thickness of the developed composites was approximately 2 mm. Shape memory SCF/SBS/LLDPE composites with short glass fiber weight fractions of 3.0 wt%, 6.0 wt%, 9.0 wt%, 12.0 wt% and 15.0 wt% were fabricated in the same way. For comparison, a pure SMP specimen was also cured under the same conditions.



Scheme 1 Cross-linked SBS/LLDPE blends

### Methods

#### Sol/gel analysis

To estimate the degree of cross-linking in SBS/LLDPE blends, the sol/gel analysis was performed for the samples. Triplicate samples with mass of about 50 mg ( $m_0$ ) were cut from the samples, and copper net was used

to wrap the samples with the combined mass denoted as  $m_1$ . Moreover, benzene was chosen as the solvent, and then the sample-solvent mixture was heated to 120 °C for 72 h. The swollen gels were then removed from the vials and washed with acetone to remove residual solvent. At last, the samples were dried in oven for 6 h, and the dried samples were weighed again ( $m_2$ ), gel fractions ( $g$ ) were calculated according to Eq. (1)

$$g = (m_2 - m_1)/m_0 \times 100\% \quad (1)$$

#### *Mechanical properties*

Tensile test was carried out at room temperature on a tensile test instrument (SANS Power Test v3.0, Shenzhen SANS Material Test Instrument Co. Ltd., China) according to ASTM D412. The sample for tensile test was dumbbell-shaped, with the length of 115 mm, the width of 50 mm and the thickness of 2 mm. The strain rate was 100 mm/min. The tensile strength and elongation at break were recorded.

#### *Differential scanning calorimetry (DSC)*

The melting temperature ( $T_m$ ) of the sample was determined with differential scanning calorimetry (DSC, Pyris 1, Perkin Elmer, USA). Samples of about 5.0 mg were heated from 0 °C to 130 °C at a constant rate of 10 K/min, followed by a cooling cycle with the same rate.  $T_m$  was determined by the heating cycle.

#### *Dynamic mechanical analysis (DMA)*

For DMA test, sample was cut to dimensions of 2 mm × 12 mm × 30 mm, and the edges of the sample were wet sanded with 600 grit sandpaper. DMA was performed in single cantilever clamping fixture and run on a TA Q800 machine. A small dynamic load at 1 Hz was applied to a platen and the temperature was ramped from -10 °C to 150 °C at a rate of 3 K/min. The amplitude was set to be 10 μm.

#### *Scanning electron microscopy (SEM)*

SEM (INCA X-ACT) was used to observe the cross-sectional morphology of the composites.

#### *Shape memory behavior test*

Rectangular specimen (100 mm × 10 mm × 2 mm) was used to evaluate the shape memory of the SCF/SBS/LLDPE composites. The shape memory model was shown in Fig. 1, and the shape recovery test was performed as following: (1) The specimen was heated up to the deformation temperatures in an oven and held for 10 min; (2) The specimen was bent into U shape under constant force; (3) The U shaped specimen was then quickly removed from the oven and dipped into a cold water bath with a constant external force; (4) Heating up the specimen to deformation temperature (10 K/min), the shape recovery process was observed and the shape recovery angle was recorded. When the specimen did not change, the recovery time was recorded. Five specimens, for each sample with a given amount of short glass fiber, were measured to get an average recovery time. The shape recovery speed corresponding temperature was defined as  $\theta/t$ , and the shape recovery speed as  $(\theta_i - \theta_f)/\theta_i \times 100\%$ .

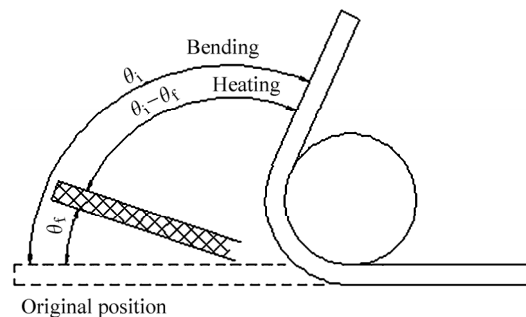


**Fig. 1** Shape memory model

## RESULTS AND DISCUSSION

### Gel Content

The crosslinking degree of SBS/LLDPE blends is a key factor to influence the shape memory effect of SCF/SBS/LLDPE composites. Therefore, it is necessary to analyze the effect of SCF on gel content of the composites. As seen from Fig. 2, with the crosslinking degree of the SBS/LLDPE blends of 63.82%, the gel content of the SCF/SBS/LLDPE composites decreased first with the SCF content, and then it was gradually leveled off at 12.0 wt% SCF. This indicates that the SCF has negative effect on the crosslinking degree of the SCF/SBS/LLDPE composites. This is due to the fact that SCF hinders the free movement of the molecular chains, and reduces the probability that the molecules are linked to each other.

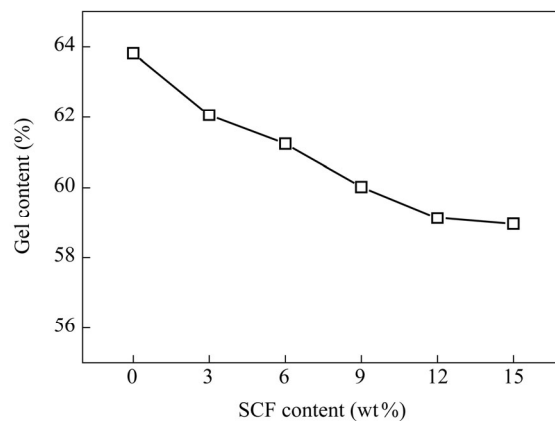


Fig. 2 Gel content of SCF/SBS/LLDPE composites

### DSC Analysis

To study the shape memory performance of SBS/LLDPE blends, we first ascertained the shape memory transition temperature, based on which the shape recovery temperature was chosen<sup>[16, 17]</sup>. The shape memory transition temperature of SCF/SBS/LLDPE composites was determined by DSC (Fig. 3). The endothermic peak corresponding to the melting temperatures of the LLDPE was taken as the shape memory transition temperature of SCF/SBS/LLDPE composite. Figure 3 illustrates that the shape memory transition temperature of the composites was about 110 °C and the peak moved to a higher temperature with an increase in the SCF content. Note that the SCF as fillers will hinder the movement of molecular chains. This is considered as friction interaction that would help SMP composites to resist external loading, resulting in the improvement of melting temperature.

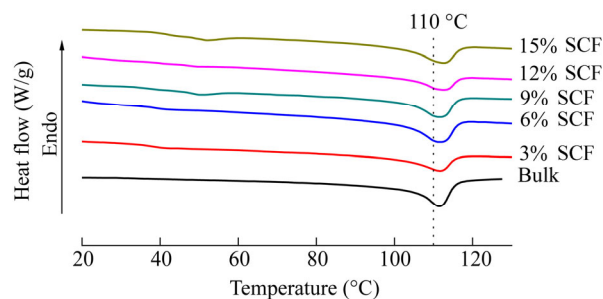
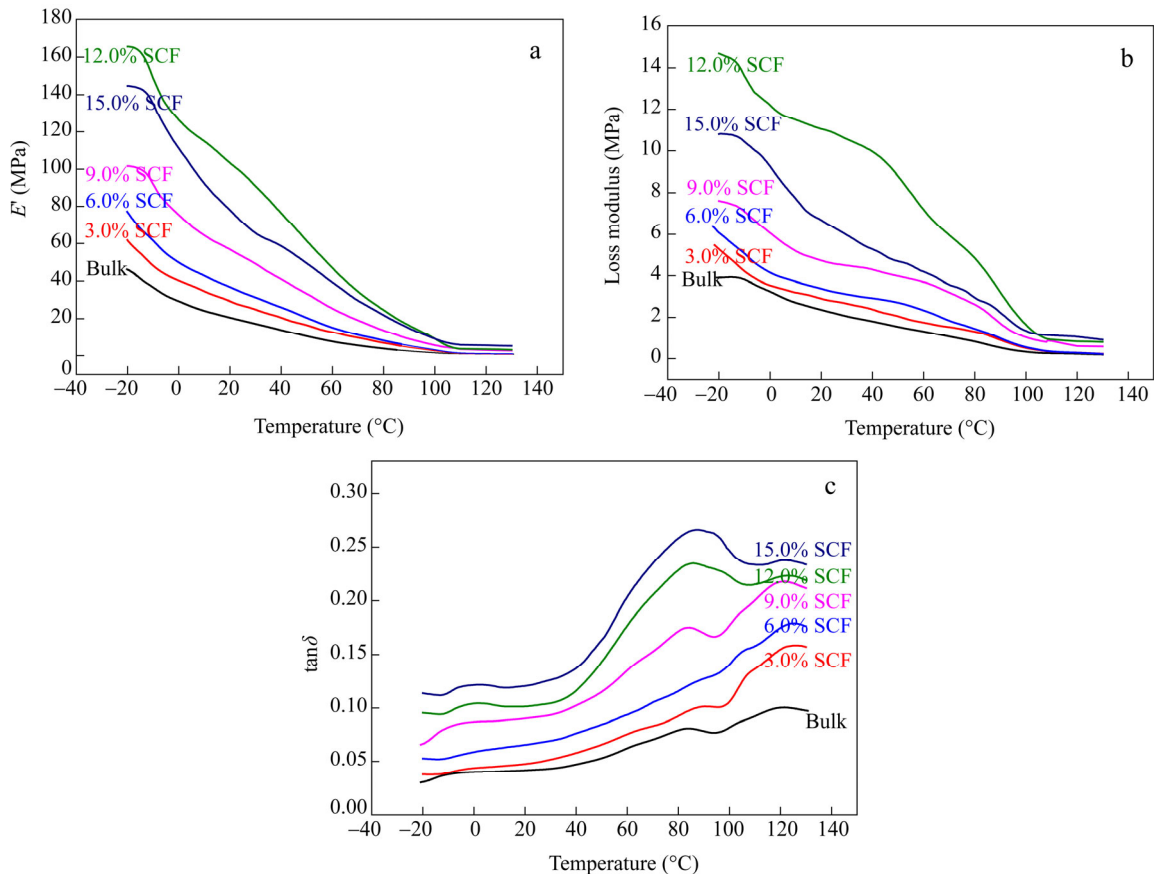


Fig. 3 DSC thermograms of SCF/SBS/LLDPE samples with different SCF contents

### DMA Analysis

Viscoelastic properties of the samples were investigated by DMA in single cantilever clamping mode. A high glassy state modulus provides the materials high shape fixity. This arises from the fact that high glassy modulus is indicative of high cohesive energy, which leads to minimized propensity for creep related shape change. High glassy modulus is not always mandatory for high shape fixity but is desirable, whereas the high rubbery modulus implies high elastic recovery at high temperature<sup>[18]</sup>. The profiles of storage modulus, loss modulus and loss tangent for the shape memory SCF/SBS/LLDPE composites are shown in Fig. 4. As seen in Fig. 4, the modulus decreased rapidly as the composites were heated through the switching transition regime, and this decrease occurred because of the increased mobility of the polymer segments, thereby inducing the shape memory actuation. The molecular inhomogeneity of the composites was related to the breadth of loss modulus, which was the full width at half maximum of the  $\tan\delta$  peak. This fell in a temperature breadth of 100 °C, a moderately wide transition range. This indicates that the shape memory properties were prominent in this regime and was effectively performed within this wide temperature range. From the curves of  $\tan\delta$ , two peaks were seen. The first at about 90 °C was the glass transition temperature of the hard phase (polystyrene) in the SBS, and the second at about 110 °C was the melting temperature of the crystalline region in the LLDPE, which was also the shape memory transition temperature of the SCF/SBS/LLDPE composites.



**Fig. 4** Dynamic mechanical properties of the SCF/SBS/LLDPE composites: (a)  $E'$ , (b) loss modulus and (c)  $\tan\delta$

At the same time, the glassy modulus was closely related to the shape fixity as the deformed shape was fixed upon cooling to glassy state while the rubbery modulus to shape recovery to the original shape were recovered in rubbery state. Figure 4 indicates that the storage modulus increased as the SCF content increased,

but it decreased slightly when the SCF content was increased to above 12.0 wt%. Normally, the storage modulus of specimens would increase by SCF reinforcement. However, the dispersion of SCF in the SBS/LLDPE blends would be uneven when the SCF content increased to a certain amount. The clustering of the SCF would exist in the SBS/LLDPE blends, which might prevent each fiber to act independently and to contribute to load sharing. Meanwhile, it was noted that high SCF content resulted in void formation. The void between the matrix and SCF may lead to the load bearing capacity of composites decreasing. Therefore, the storage modulus of the composites increased with the increase of SCF and decreased slightly when SCF content reached 12 wt %.

Figure 5 shows the microstructures of the specimen with different content of SCF. It was found that, with the increase in SCF content, the surface of the composites became rough, and the agglomeration was obvious when the SCF content reached 15 wt%.

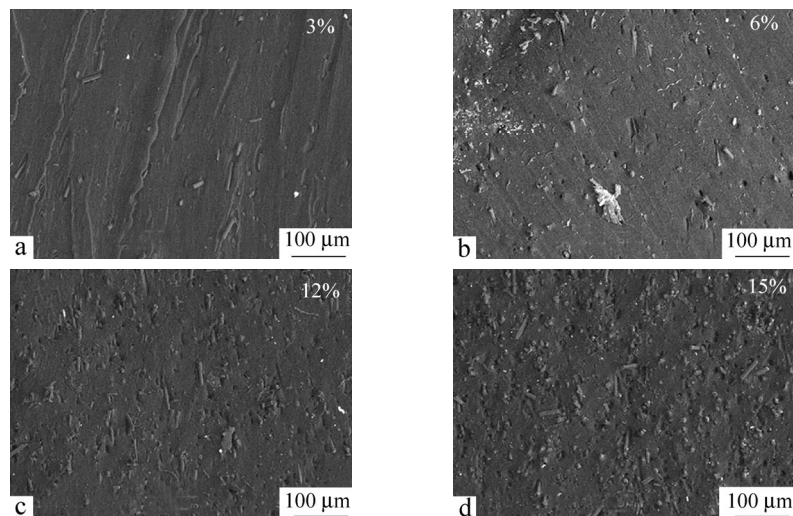


**Fig. 5** SEM images of the composites with different SCF contents: (a) 3%, (b) 6%, (c) 12% and (d) 15%

#### *Mechanical properties*

The tensile property is one of the most important indicators to the mechanical property of SCF/SBS/LLDPE composites. The relationship between mechanical properties and SCF content is illustrated in Fig. 6, where each sample was characterized by tensile tests at room temperature. From Fig. 6(a), the following was observed: (i) the tensile modulus of SCF/SBS/LLDPE composites increased with SCF content but decreased when the SCF content reached 15 wt%. A tensile strength of about 12.5 MPa was detected for the bulk specimen without SCF; (ii) it is remarkable that the elongation at break decreased with increase in SCF content for all specimens. Considering the SCF as the reinforcement, the tensile strength of the composites would increase. However, the SCF would be offset by the uneven dispersion of fiber reinforcement. Moreover, higher fiber content would lead to the formation of more voids, which would result in micro-crack formation under loading and reduce therefore the tensile strength. The strain-stress curves of the SCF/SBS/LLDPE composites are illustrated in Fig. 6(b). The results show that the tensile modulus, yield stress and tensile strength of SMP was improved with the incorporation of SCF and the elongation at break was decreased at the same time. The incorporation led to overall reinforcing effect in tensile strength, yield stress, tensile modulus and elongation at break of SMP. Similar results have been reported<sup>[19, 20]</sup>.

#### *Shape memory behavior analysis (bending test)*

The base of the shape memory mechanism of the SBS/LLDPE blends is that there are two phase morphology in the blends. SBS and crosslinking network in the blends are the fixed phase and the crystalline region in the LLDPE is the reversible phase. Qualitatively, the shape memory behavior of SCF/SBS/LLDPE composites was estimated by bending test at the shape memory transition temperature. The shape memory effect of specimen



with 6.0 wt% of SCF is shown in Fig. 7. Starting from the original shape, the specimen was deformed into U shape in the oven. Upon cooling under load, the deformed temporary shape was fixed. By placing the specimen in an oven at 110 °C, full recovery could be observed after only 200 s.

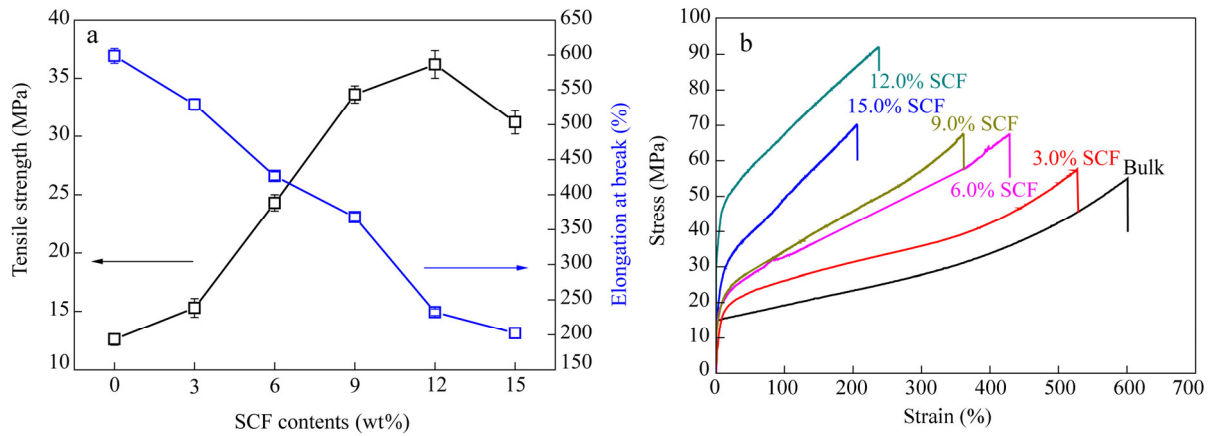


**Fig. 6** Mechanical properties of the SCF/SBS/LLDPE composites: (a) tensile strength and elongation at break, (b) strain-stress

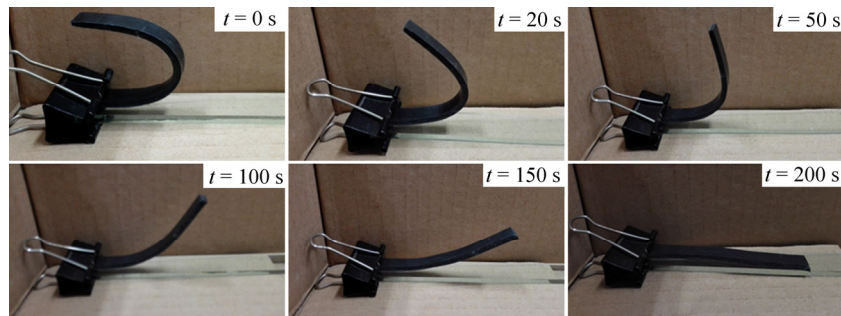


**Fig. 7** Shape memory test of SCF/SBS/LLDPE composite with 6.0 wt% of SCF at 110 °C

Figure 8 illustrates the relationship between the recovering angle and recovering time of the bulk, 3.0 wt%, 6.0 wt%, 9.0 wt% and 12 wt% samples. The results indicated that full recovery was observed after only several minutes at  $T_m$ . Therefore, the shape recovery ratio of almost 100% was obtained for the bulk specimen and those with SCF content of 3.0 wt%, 6.0 wt%, 9.0 wt% and 12 wt%, demonstrating excellent shape memory performance for all the SCF/SBS/LLDPE composites. Moreover, SCF did not impose significant effect on the shape memory property of the developed composites when SCF content between 3.0 wt% to 12.0 wt%, though the shape recovery time significantly increased with the increased SCF content because the stiffness of the composites was increased at the same time. Meantime, as shown in Fig. 8, the slope of the curve was generally larger with recovering angle between 60° and 120° in comparison with the same slope with recovering angle above 120°. This meant a fast shape recovery at earlier stage. However, Figure 8 shows a relatively low recovery rate for the specimens at the initial stage as at the final stage. At the initial stage, the release of the stored strain energy was followed by heavy friction among segments, which would cause decreased shape recovery rate. When the stored strain energy was released largely at the anterior stage; the shape recovery rate became slow at the final stage. The specimen with 15 wt% of SCF was not used as a shape memory material because fully recovery was not possible for this specimen.

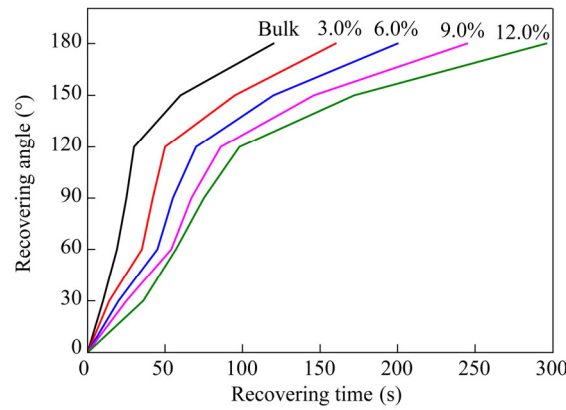


Fig. 8 Relationship between recovering angle and recovering time of SCF/SBS/LLDPE composites at  $T_m$

The shape memory effects of the SCF/SBS/LLDPE composites are presented in Table 1. From Table 1, it was found that the shape fixity rate and shape recovery time of the SCF/SBS/LLDPE composites increased with the SCF content. This was attributed to the SCF in the fixed phase, which was helpful to improve the shape fixity rate of the SCF/SBS/LLDPE. However, the shape recovery ratio of the composites decreased with the SCF content. This was because that SCF did not have shape memory effect, thus SCF imposed negative effect on the molecular chains movement to their initial shape. Meanwhile, the shape recovery time also increased with the SCF content, which implied that the shape recovery rate decreased with increasing SCF content.

Table 1. Shape memory effect of SCF/SBS/LLDPE composites

Sample	Shape fixity rate (%)	Shape recovery ratio (%)	Shape recovery time (s)
Bulk	95.2	100	120
3.0 wt% SCF	96.5	99.8	173
6.0 wt% SCF	97.3	99.5	200
9.0 wt% SCF	98.7	99.2	232
12 wt% SCF	99.2	98.9	274

Figure 9 shows the effect of cycling times on recovery ratio of SCF/SBS/LLDPE composites. It was found that the shape recovery ratio of composites decreased slightly with increasing cycling times. This was attributed to the accumulation of plastic deformations in the composites, which was inevitably to occur during the recovery process. Moreover, the shape recovery ratio slowly decreased with the SCF content because an increase in SCF content should lead to an increase in stiffness of the materials, thus to reduce the plastic deformation of the specimen.

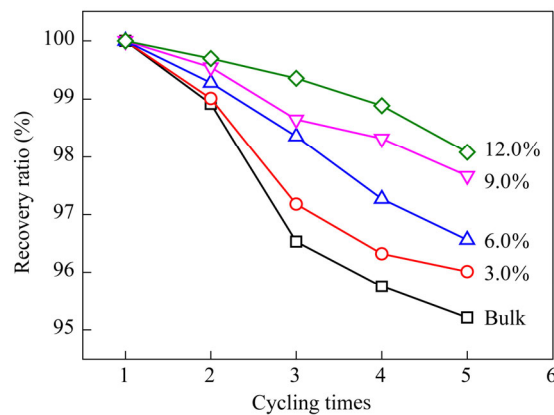


Fig. 9 Effect of cycling times on recovery ratio of SCF/SBS/LLDPE composites with different SCF content



## CONCLUSIONS

Shape memory SBS/LLDPE composites, incorporated with different amounts of SCF, were fabricated. These composites were of excellent processability compared with other composites. SCF filler did not cause any change in the shape memory transition temperature of the composites. The large amount of SCF significantly improved the mechanical property of the composites while not damaging the shape memory performance. When SCF content was less than 15.0 wt%, the SCF/SBS/LLDPE composites showed excellent shape memory properties, and full recovery was observed after only several minutes at shape memory temperature. The shape recovery time and shape recovery ratio slightly increased with increasing SCF content. However, the shape recovery ratio decreased with increasing cycling time.

## REFERENCES

- 1 Wang, Y.K., Zhu, G.M., Cui, X.P., Liu, T.T., Liu, Z. and Wang, K., *Colloid Polym. Sci.*, 2014, 292(9): 2311
- 2 Wang, Y.K., Zhu, G.M., Tang, T.S., Xie, J.Q., Liu, T.T. and Liu, Z., *J. Polym. Res.*, 2014, 21(4): 2
- 3 Wang, Y.K., Zhu, G.M., Tang, T.S., Liu, T.T., Xie, J.Q. and Ren, F., *J. Appl. Polym. Sci.*, 2014, 13(17): 40691
- 4 Wang, Y.K., Zhu, G.M., Xie, J.Q., Men, Q.N., Liu, T.T. and Ren, F., *J. Polym. Res.*, 2014, 21(8): 515
- 5 Liu, Y.J., Lv, H.B., Lan, X., Leng, J.S. and Du, S.Y., *Compos. Sci. Technol.*, 2009, 69(13): 2064
- 6 Zhao, Q., Qi, H.J. and Xie, T., *Prog. Polym. Sci.*, 2015, 49: 80
- 7 Zhen, W.M., Zhao, Y., Wang, C.C., Ding, Z., Purnawali, H., Tang, C. and Zhang, J.L., *J. Polym. Res.*, 2012, 19(9): 9952
- 8 Liu, C., Qin, H. and Mather, P.T., *J. Mater. Chem.*, 2007, 17(16): 1544
- 9 Zheng, N., Fang, G.Q., Cao, Z.L., Zhao, Q. and Xie, T., *Polym. Chem-UK.*, 2015, 6(16): 3048
- 10 Wang, C.C., Huang, W.M., Ding, Z., Zhao, Y. and Purnawali, H., *Compos. Sci. Technol.*, 2012, 72(10): 1178
- 11 Bijju, R. and Nair, C.P.R., *J. Polym. Res.*, 2013, 20(2): 82
- 12 Voit, W., Ware, T. and Gall, K., *Polymer*, 2010, 51(15): 3555
- 13 Zhang, J.N., Ma, Y.M., Zhang, J.J., Xu, D., Yang, Q.L., Guan, J.G., Cao, X.Y. and Jiang, L., *Mater. Lett.*, 2011, 65(23): 3639
- 14 Lv, H.B., Yu, K., Sun, S.H., Liu, Y.J. and Leng, J.S., *Polym. Int.*, 2010, 59(6): 766
- 15 Lan, X., Liu, Y.J., Lv, H.B., Wang, X.H., Leng, J.S. and Du, S.Y., *Smart. Mater. Struct.*, 2009, 18(2): 024002
- 16 Guo, W.S, Shen, Z.L., Guo, B.C., Zhang, L.Q. and Jia, D., *Polymer*, 2014, 55(16): 4328
- 17 Wang, W.X., Liu, D.Y., Liu, Y.J., Leng, J.S. and Bhattacharyya, D., *Compos. Sci. Technol.*, 2015, 106: 22
- 18 Kim, B.K., Lee, S.Y. and Xu, M., *Polymer*, 1996, 37(26): 5789
- 19 Amirian, M., Chakoli, A.N., Sui, J.H. and Cai, W., *J. Polym. Res.*, 2012, 19(2): 9777
- 20 Ohki, T., Ni, Q.Q., Ohsako, N. and Lwamoto, M., *Compos. Part A-Appl. S.*, 2004, 35(9): 1069